

## GROUND BASED MEASUREMENTS OF STRATOSPHERIC OZONE IN ANTARCTICA

A.V. NEMUC<sup>1</sup>, R.L. DEZAFRA<sup>2</sup>

<sup>1</sup>*Bucharest University, Faculty of Physics, Romania  
email:anemuc@hotmail.com*

<sup>2</sup>*Institute for Terrestrial and Planetary Atmospheres,  
State University of New York at Stony Brook, N.Y., U.S.A.*

(Received June 22, 2005)

*Abstract* . Measurements of ozone in Antarctica, during 1999, will be presented and compared with 1993 and 1995 ozone observations made with the same ground-based millimeter-wave spectrometer (GBMS). High-resolution spectral observations of pressure-broadened emission line shapes from the molecular rotational transition at 277 GHz have been obtained and were deconvolved against locally measured pressure and temperature profiles to retrieve ozone mixing ratio profiles with good accuracy over the altitude range 16 to 50 km. Features common to all three annual cycles for ozone are noted and discussed, including a pronounced summer-fall decline in mid-to-upper stratospheric ozone followed by an early winter recovery, a dramatic increase of stratospheric ozone during and following the vortex breakup and a double-peaked vertical profile for the ozone mixing ratio .

*Key words*: ozone, Antarctica, measurements, stratosphere, vortex , observations.

Measurements of ozone in Antarctica

### 1. INTRODUCTION

Until a series of ground-based observations were begun with the Stony Brook Ground-based millimeter-wave spectrometer (GBMS) during 1993, no extended profiles of ozone were available in the heart of the Antarctic vortex on a continuing, regular basis through the polar winter. The GBMS has given a unique picture of ozone evolution over the pole through the mid to upper stratosphere, using data taken as frequently as every 3 days, and has revealed behavior not previously seen. We have published data from 1993 observation in [4], and a comparison of data again taken in 1995 with 1993 data in [5]. Here, we present a third year of observations taken during 1999. Most of the yearly cycle of behavior is again represented with good coverage, and comparisons can be made between these well-separated years.

### 2. APPARATUS AND DATA ANALYSIS

Data were taken with the Stony Brook GBMS two to three times per week when conditions allowed. One major equipment problem kept us from obtaining data for ~45 days starting in late September, 1999. (Days when satisfactory data were

available and analyzed are shown as triangular ticks along the lower axis of the 1999 data panel in Fig. 1). Typically, 30 minutes of integration time was required to obtain a signal/noise ratio of  $\sim 100/1$ , large enough to insure that retrieval accuracy is not noise limited. The spectral resolution is 1 MHz per channel, and the total frequency window of the spectrometer is 512 MHz. Vertical mixing ratio profiles were retrieved from the 276.923 GHz ozone rotational emission line using a modified Chahine-Twomey deconvolution technique[12,13]. The design and observing technique is described in greater detail in [7].

For these deconvolutions, we used temperature and pressure data that are a composite from daily meteorological balloons launched at the South Pole (3 to  $\sim 20$  km) and daily NCEP profiles ( $\sim 20$ -40 km, above which NCEP temperatures are unreliable over the Pole), with an extension to 60 km by fitting monthly model profiles from the COSPAR International Reference Atmosphere of 1986. The intensity of the 277 GHz ozone transition is nearly insensitive to temperature: a 10 K systematic shift over the entire atmospheric temperature profile will cause less than 1% change in emission intensity [6], so that this combination of temperature profiling is quite adequate for our purposes. Accuracy estimates covering other aspects of the instrumental and parameter uncertainties for this ozone emission line are also discussed in [6] and [4]. We will be more concerned here with time trends than in absolute accuracy, and some possible systematic errors (e.g. in the ozone line broadening parameter) contributing to overall accuracy discussed in the above references are of little consequence for this analysis.

We have improved our application of corrections that account for small amounts of self-absorption of upper stratospheric ozone line emission passing through lower ozone layers, and for geometrical viewing effects. These corrections affect the central line intensity - hence tend to improve the upper stratospheric retrieval accuracy - relative to that of the 1993 and 1995 retrievals. In the resulting 1993 and 1995 contour maps (shown in Figure. 1 with original processing), we noted that descent rates for contours in the 40-50 km range appeared to show a slower, and therefore physically unreasonable, rate of descent than contours below 40 km. In the earlier processing, a single correction factor was used throughout the winter until formation of the ozone hole after sunrise. For the present analysis, we have generated time-dependent corrections for self-absorption from short term (weekly to monthly) averages of lower altitude ozone from past retrievals and current ozonesonde data. This may be responsible for some improvement in apparent descent rates of ozone in the second half of winter, relative to expected descent rates, if ozone is considered an inert tracer during Polar darkness.

### 3. COMPARISON OF OZONE OBSERVATIONS IN 1999 WITH 1993 AND 1995 DATA

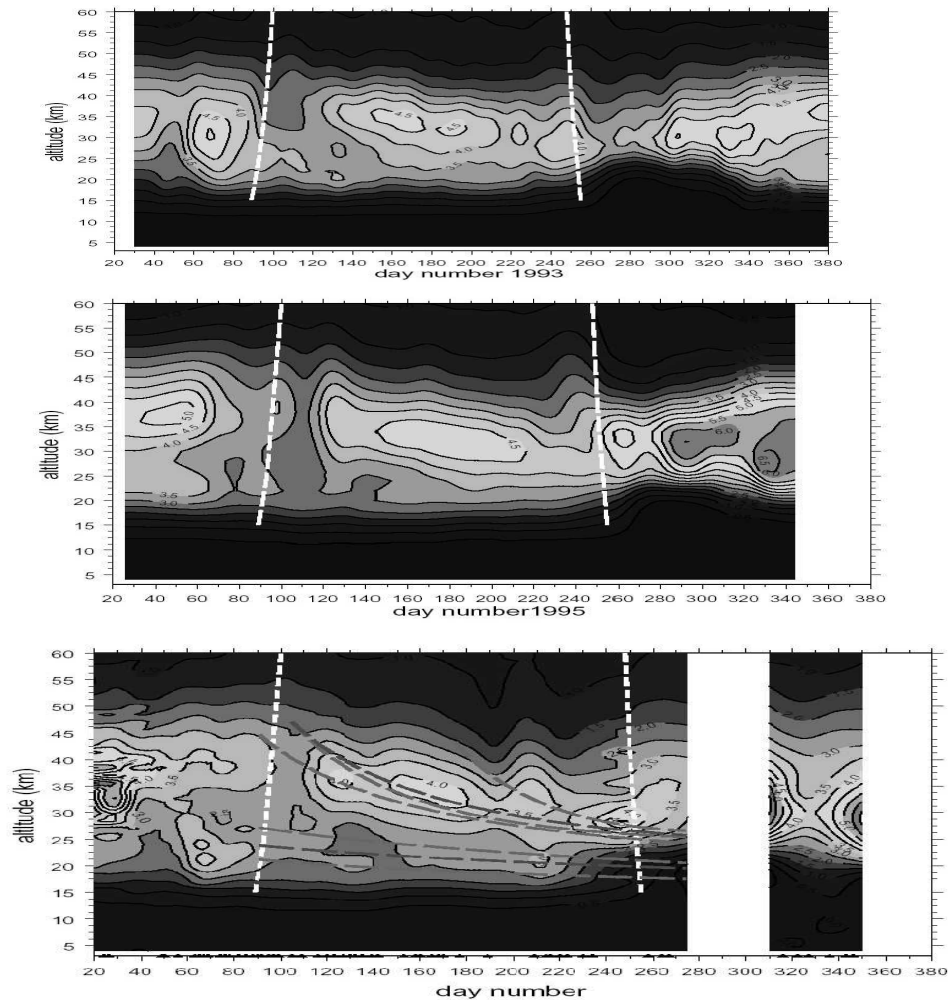


Fig. 1 - Top, middle, and lower panels show 1993, 1995, and 1999 ozone data, respectively, displayed as contour plots. Day numbers are plotted along the horizontal axes and altitude in km on the vertical axes. Slanting white dashed lines show Polar sunset and sunrise as a function of altitude. For 1999, days when usable data were obtained are indicated by triangles along the lower edge. Contours are label in ppmv, and the interval between contours is 0.5 ppmv. Heavy diagonal curves mark diabatic descent rates calculated for starting altitudes and times shown, from Rosenfield et al., [9,10].

Fig. 1 presents contour maps of ozone mixing ratios as a function of altitude and date, a comparison of 1993 and 1995 with observations taken during 1999. Most of the yearly cycle of behavior is again represented with good coverage. The maps have been derived from observations of vertical profiles over the South Pole in February 1993-January 1994, January-December 1995 and late January-December 1999. One

major equipment failure kept us from obtaining data for ~45 days starting in late September 1999.

### 3.1 Summer-fall ozone decline and winter recovery

An interesting, and we believe hitherto unstudied, feature of mid-stratospheric Antarctic ozone is the rapid fall-off in mixing ratio seen in all panels of Figure 1 beginning before sunset, followed by a return to larger mixing ratios after several weeks. This was commented in [5], but now a third, well separated, year of data confirms this as 'standard' behavior in need of further study. In a future study we will try to investigate this feature using a combination of GBMS data and data taken with the Upper Atmosphere Research Satellite (UARS) Microwave Limb Sounder (MLS) instrument.

### 3.2 Descent of ozone isopleths throughout the stratosphere during winter

Fig.1 clearly shows descent of ozone isopleths throughout the stratosphere during winter. Various theoretical and experimental studies have been made in recent years to determine typical rates of descent within the Antarctic vortex during winter. Vortex descent has the important effect of altering profiles of mixing ratio versus altitude for various species, and therefore altering the speed and end-point for various chemical reactions between species, due to their (frequently) strong dependence on pressure and temperature.

Although  $O_3$  is essentially inert chemically in the middle-atmospheric winter darkness, it was found that descent traced by constant mixing ratio contours of  $O_3$  versus time showed physically incorrect slower descent in the upper stratosphere than in the middle stratosphere in 1993. We have now extended the observations to the austral winter of 1999. Descent rates seem faster at high altitudes in the mid-winter, in the 1999 contour plot (Fig.1 lower panel). When contrasted, however, with typical calculated diabatic descent rates from the South Polar vortex model of Rosenfield et al. [9], (shown as overlaid purple curves in the top panel of Fig. 9), it is clear that upper stratospheric ozone still does not show descent in agreement with calculated rates for vertical air motion.

Rosenfield et al. [10] have estimated diabatic descent rates from various altitudes within the polar vortices by calculating diabatic cooling from UKMO assimilated temperature fields for 1992 and 1993, considering the vortices as isolated systems without cross-boundary transport.

More recently, Rosenfield et al. [10] have recalculated polar diabatic descent rates using back trajectory calculations on air parcels over periods up to seven months in an effort to determine average origins and thermal history of air reaching the vortex core by mid-winter. They conclude that descent predicted by this technique is always slower than descent rates calculated on the basis of an 'isolated' vortex, because horizontal motion and variation in heating (cooling) rates with latitude and longitude reduce the time-integrated rates of cooling. The use of multi-month back trajectories,

even though used only to establish average origins and motions, may be of questionable validity however, and it is probably best to take the original [9] and more recent [10] calculations of Rosenfield et al. to represent approximate extremes within which real vortex behavior may lie.

In an unpublished analysis we made a comparison between experimental descent rates inferred from  $N_2O$ ,  $O_3$ , and  $HNO_3$  isopleths from 1999 South Pole data. Upper stratospheric  $O_3$  appear to descend more slowly than mid-stratospheric  $O_3$ , and in neither case approach agreement with theory, in contrast to  $N_2O$ . Mid-to-upper stratospheric  $HNO_3$  appear to show a much more rapid descent than  $O_3$  within the same altitude range during mid to late winter, but both species, once formed, are supposed to be chemically inert the winter darkness. Accepting the latter premise, one must invoke a dynamical explanation. Different species may be expected to show different apparent descent rates if they have different mixing ratio gradients across the vortex boundary and if cross-boundary transport is significant, as was also suggested by other researchers mentioned in the introduction [e.g. 1,2,3,11]. Advection of air at higher altitudes across the vortex boundary will introduce air richer in ozone than air that has descended within an isolated vortex. This air, carried along ~constant potential temperature surfaces over periods of several days and mixing with core air, will sustain larger  $O_3$  mixing ratios versus altitude than would otherwise be present in an isolated vortex.

### 3.3 Double-peaked profiles

Double-peaked profiles observed in 1993 and 1995 were again found in most 1999 profiles except for the 'ozone hole' period, when chemical depletion eats away the lower peak, and winter time, when the lowest peak become very thin (as seen in high resolution ozonesonde profiles) and therefore not well retrieved by our deconvolution technique. As an example, in Fig. 2 we show typical mm-wave profile retrievals overlaid with the once-weekly NOAA South Pole balloon-sonde data for the month of March 1999. Although three ozonesondes reached ~30 km (the fourth failed at ~13 km), none go high enough to reveal the significantly greater mixing ratio peak found a little below 40 km. The "double-peak" structure found in mm-wave retrievals is generally too weak to stand out in Fig. 1, where fairly coarse gridding has been used to create the contour maps in order to emphasize large scale, long-term trends in vertical behavior. This double-peaked or layered vertical distribution holds important information about seasonal stratospheric transport and chemistry at the heart of the Antarctic vortex [4].

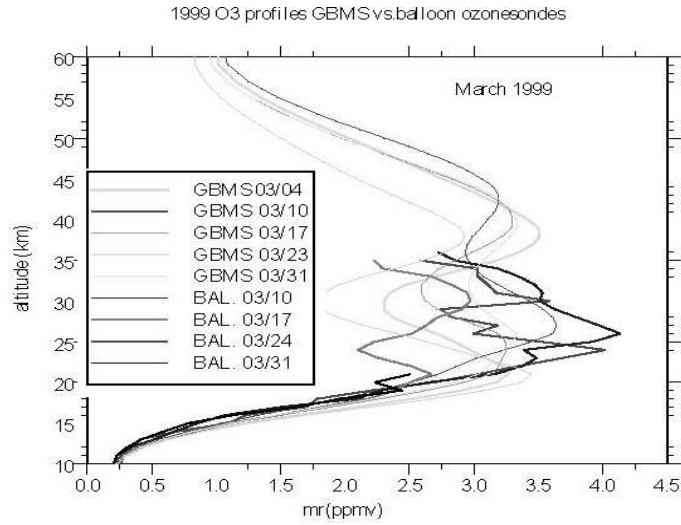


Fig. 2 - GBMS ozone profile retrievals overlaid with the once-weekly NOAA South Pole balloon-sonde data for the month of March 1999.

Cheng et al.[4] found a good overall agreement in total column densities between observations made with the Stony Brook GBMS, NOAA ozonesondes and the Dobson spectrometer at the South Pole in 1993. In Fig. 3 we now offer a direct comparison between three years of measurements made with the same instrument. We note lowest ozone records during fall and winter 1999 and late ozone hole recovery during spring 1999, which have also been seen in the NOAA balloon ozonesonde yearly comparison at the South Pole (NOAA Report-Southern Hemisphere Winter Summary, available online at: <http://www.cpc.ncep.gov> with location products/stratosphere/winter-bulletins at the South Pole).

### 3.4 Total column density versus time

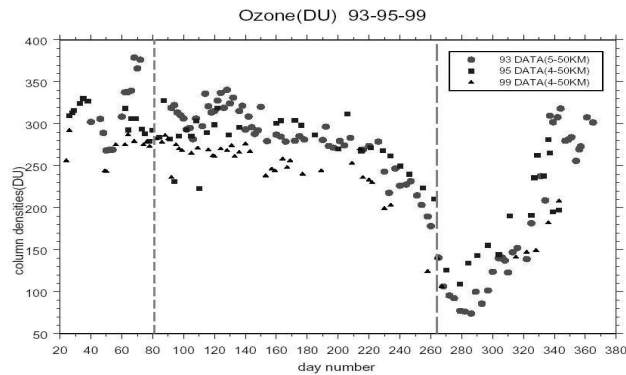


Fig. 3 - Total ozone column in Dobson units in time for 1993, 1995, 1999. Dashed lines approximate the polar sunset and sunrise.

Contour plots do not show the ozone hole as a very prominent feature. To illustrate more clearly the degree to which the total ozone column is depleted, column density measurements were made by integrating the retrieved mixing ratio profiles from 4 to 50 km (surface altitude at the Pole is 2.8 km), for 1993, 1995, and 1999. They are plotted in Fig. 3. It is clear that ozone column density starts to decrease steadily beginning about day 220 (August 8), more than 40 days before Polar sunrise (dashed vertical line at ~day 264). By sunrise, it has dropped to roughly half its mid-winter value. The decline continues until maximum depletion has been reached by the end of the first week in October (~day 280).

The contour plots for 1993, 1995 and 1999 (Fig. 1) show that the rapid pre-sunrise decrease in column ozone takes place below 25 km, within the altitude range covered by the springtime 'ozone hole'. This "early" onset of rapidly declining ozone is comparable to the timing seen in Manney et al. [8] from UARS Microwave Limb Sounder measurements averaged over a PV-equivalent latitude band from  $\sim 60\text{-}80^\circ$  S, considerably further from the Pole. A comparison of 12-day back trajectories at  $\sim 20$  km for air passing over the Pole shows relatively little to distinguish July or early August trajectories from those in the latter half of August, when depletion is clearly underway, but when solar exposure along the trajectories is compared, the difference is evident.

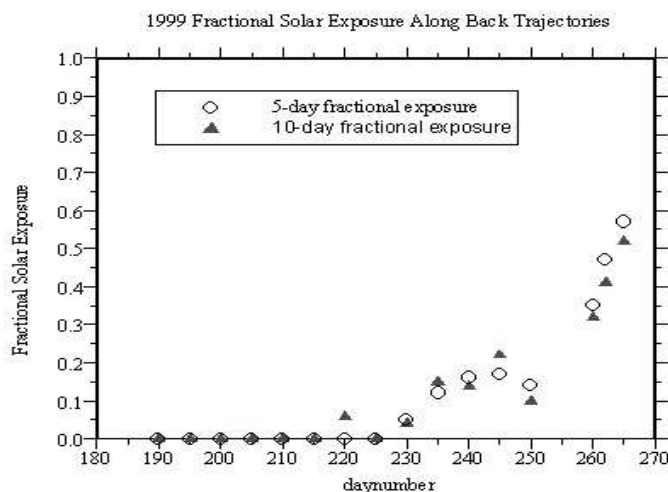


Fig. 4 - Fractional solar exposure time during the previous 5 and 10-day periods for various days in the winter and spring of 1999.

Fig. 4 shows fractional solar exposure time during the previous 5 and 10-day periods for various days in the winter and spring of 1999. Solar exposure time clearly correlates well with the onset of ozone depletion in air passing over the pole after ~day 220 (August 8), and as little as ~20-24 hours of exposure to sunlight appears to cause noticeable ozone depletion. In summary the early onset of ozone depletion

shown by air over the Pole is again evidence of rapid transport and mixing of air from more northerly sunlit regions of the vortex.

*Acknowledgments.* This research was supported by NASA through Grant NAG54071 and by the National Research Foundation through Grant OPP9705667. We thank Terry Deshler for access to the University of Wyoming ozonesonde measurements over McMurdo Station in 1993. South Pole ozonesonde measurements were obtained from NOAA, and the GBMS data were obtained through the dedication and skill of Curtis Trimble, who wintered over at the Pole to acquire this data

#### REFERENCES

1. D. R. Allen et al., Antarctic polar descent and planetary wave activity observed in ISAMS CO from April to July 1992, *Geophys. Res. Letters*, 27, 665-668, 2000.
2. J. Austin et al., Mid stratospheric ozone minima in Polar Regions, *Geophys. Res., Lett.*, 22, 2489-2492, 1995.
3. J. T. Backmeister et al., Descent of long-lived trace gases in the winter polar vortex, *J. Geophys. Res.*, 100, 11,669-11,684, 1995.
4. D. Cheng, R. L. de Zafra, C. Trimble, Millimeter wave spectroscopic measurements over the South Pole, 2, An 11-month cycle of stratospheric ozone observations during 1993-94, *J. Geophys. Res.*, 101, 6781-6793, 1996.
5. D. Cheng, S. Crewell, U. Klein, R.L. de Zafra, R.A. Chamberlin, Millimeter wave spectroscopic measurements over the South Pole, 4, O<sub>3</sub> and N<sub>2</sub>O during 1995 and their correlations for two quasi-annual cycles, *J. Geophys. Res.*, 102, 6,109-6,116, 1997.
6. B. J. Connor, J. W. Barrett, A. Parrish, P. M. Solomon, R. L. de Zafra, M. Jaramillo, Ozone over McMurdo Station, Antarctica, Austral Spring 1996: Altitude profiles for the middle and upper stratosphere, *J. Geophys. Res.*, 92, 13221-13230, 1987.
7. R. L. de Zafra, The ground-based measurement of stratospheric trace gases using quantitative millimeter wave emission spectroscopy, in *Diagnostic Tools in Atmospheric Physics*, Proceedings of the International School of Physics "Enrico Fermi", Course CXXIV, pp. 23-54, Varenna, 1993; Societa Italiana di Fisica, Bologna, 1995.
8. G. L. Manney, R. W. Zurek, A. O'Neill, R. Swinbank, On the motion of air through the stratospheric polar vortex, *J. Atmos. Sci.*, 51, 2973-2994, 1994.
9. J. E. Rosenfield, P. A. Newman, M. R. Schoeberl, Computations of diabatic descent in the stratospheric polar vortex, *J. Geophys. Res.*, 99, 16,677-16,689, 1994.
10. J. E. Rosenfield, M. R. Schoeberl, Studies of fall to spring Arctic and Antarctic polar vortex descent, Proceedings of the Quadrennial Ozone Symposium, Sapporo, 2000, 615-616, 2000.
11. S. E. Strahan, J. E. Nielsen, M. C. Cerniglia, Long-lived tracer transport in the Antarctic stratosphere, *J. Geophys. Res.*, 101, 26,615-26,629, 1996.
12. S. Twomey, *Introduction to the mathematics of inversion in remote sensing and indirect measurements*, Elsevier Pub., Amsterdam, 1977.
13. S. Twomey, B. Herman, Rabinoff, An extension of the Chahine method of inverting the radiative transfer equation, *J. Atmos. Sci.*, 34, 1,085-1,090, 1997.